NATIONAL BUREAU OF STANDARDS REPORT

NBS PROJECT
25106-11-2510461

August 30, 1965

NBS REPORT
8870

RECOMBINATION STUDIES IN THE AFTERGLOW OF A HELIUM, BRUSH-CATHODE PLASMA

Earl R. Mosburg, Jr.

Radio Standards Laboratory

National Bureau of Standards,

Boulder, Colorado

U.S. DEPARTMENT OF COMMERCE

NATIONAL BUREAU OF STANDARDS

TABLE OF CONTENTS

Recombination Studies in the Afterglow of a Helium, Brush-Cathode Plasma

Earl R. Mosburg, Jr.

Studies of the time dependence of atomic and molecular light intensities, electron density, atomic metastable densities, and electron temperature have allowed the determination of the He^+-electron recombination coefficient as a function of electron density and temperature. The results are in reasonable agreement with the theory of collisional-radiative recombination. The mechanisms controlling metastable densities and heating of the electron gas are discussed. In particular, the disappearance of the 2^3S metastable atom seems best explained in terms of collisional de-excitation by electrons with a cross section of the order of 10^{-15} cm^2.

Key Words: Brush-cathode plasma, Helium Afterglow and Recombination coefficient.

INTRODUCTION

In earlier experiments,[1] using pulsed microwave cavities or waveguides, the observed time dependence of the electron density was used to acertain the degree to which the loss processes were dominated by electron-ion volume recombination and, simultaneously, to determine the value of the recombination coefficient, itself from a plot of $1/n(t)$ vs. t. It has since been shown[2] that, in the presence of diffusion, linearity of a $1/n(t)$ vs. t plot is neither a guarantee of recombination control nor a good measure of the recombination coefficient, unless the region of linearity is at least a factor of about ten. Even in cases where this criterion is met, there are other uncertainties. In general, the radial

distribution of electron density was surmised rather than measured and was probably time dependent. This introduces uncertainty into the interpretation of the frequency shift of the cavity in terms of the spacial average of the electron density. There are, moreover, serious limitations to the electron density region over which the cavity technique can be applied.[3] Purity of the gas was an additional problem and, for a while, the measured recombination coefficients became progressively lower as the purity was improved. In all of these early experiments, a dependence of the assumed two-body recombination coefficients on electron density was neither allowed for nor found experimentally. For helium, the theoretical picture was further obscured by the assumption that electron loss proceeded primarily by dissociative recombination of the He_2^+ ion,[4] a belief that has persisted until very recently.

If the above uncertainties were disconcerting when only two-body recombination was to be considered, they are much more so now after the development of the theory of collisional-radiative recombination,[5] since this theory predicts a recombination coefficient which is in most cases strongly dependent on both electron density and electron temperature. Measurements of the recombination coefficient without fairly precise, correlated measurements of the electron density and electron temperature are, therefore, meaningless.

Recent experimental and theoretical developments have shown that recombination in helium cannot be interpreted in terms of a dissociative mechanism.[6] Other recent work[7, 8] is in reasonable agreement[9] with the theory of collisional-radiative recombination but further experimental confirmation is clearly needed.

In this experiment, an attempt is made to remove some of the difficulties associated with previous measurements by moving to a regime where the loss rates are more strongly dominated by recombination and by using a more optimum geometry, in this case a

cylinder of sufficient diameter that measurements of radial dependence become relatively easy, and of sufficient length that the end effects can be neglected. The newly developed brush cathode [10] was used because it provides a high energy ($\sim$ 3 KeV) electron beam excitation of the plasma, resulting in a source function which is constant over the volume.[11] The result is an experimental situation which is very well suited to the measurement of recombination. The combination of high electron density ($\sim 10^{12}$ cm^{-3}), low electron temperature ($\sim$ .05 to 0.1eV) and relatively large size (8-cm diameter x 50-cm length) assures both a rather high degree of recombination control and the possibility of determining the radial distribution of the light intensity. Furthermore, the ratio of [He (2^3S)] to the electron density, n, is relatively low (1:4 to 1:10) and there is proportionally less influence of the 2^3S metastables during the afterglow. A procedure of analysis is here presented which allows the calculation of the recombination coefficient, from the experimental line intensity and electron density measurements, and in the presence of ambipolar diffusion, without any assumption as to the specific dependence of the recombination coefficient on electron density.

EXPERIMENTAL PROCEDURE

Figure 1 shows the plasma tube including two brush cathodes, which are operated at high negative potential, and two grounded anodes. The region of the plasma subjected to study was midway between the two anodes and was therefore free of fields except for the space charge field set up by ambipolar diffusion to the wall. The excitation current, which could be varied between 20 mA and 100 mA, was monitored by measuring the voltage across a 1-ohm resistor connecting the two anodes to ground. The system was baked to 450° C, after which a

vacuum of $\lesssim 3 \times 10^{-10}$ torr was indicated. The system was then filled with helium, purified by allowing it to leak into a reservoir thru a heated quartz wall.[12] In filling the plasma tube from the reservoir, the pressure was measured using a capacitance manometer, calibrated against an oil manometer. Pressures of from 0.7 to 1.2 torr were used. Spectroscopically no lines were observed of neon, the major impurity in commercial helium. Any such lines present were of considerably lower intensity than the Fe I impurity lines which were observed.

The tube was pulsed 20 to 30 times per second, the excitation voltage being allowed to build up slowly so that the plasma could come to equilibrium. Thus an on-time of 3 to 5 ms was required. The voltage was then removed abruptly by the use of a thyratron. resulting in the disappearance of the excitation current within approximately 3 μs. Although the cathode voltage did not drop quite to zero and hence a slight amount of current continued to flow between cathode and anode, the power involved was very low, dropping from $\sim$ 200 W during the discharge, to less than 4×10^{-2} W, within 100 μs. and further decreasing to $<3 \times 10^{-3}$ W after 1 ms. Furthermore, due to their low mean free path, the penetration of these few low energy electrons into the center of the tube could occur only by diffusion. Thus even this small amount of power was contained within the cathode-anode regions. Ion production by this residual current was nil since a uniform drop of 30 V or less in 5 cm is incapable of producing ionization in helium at a pressure of 1 torr.

Five different types of measurement were made on the decaying plasma as a function of time. They are measurements of spectral line intensity, line intensity profile, electron density, electron temperature, and absorption of 3889 Å light. These will be discussed in turn.

The spectral line intensity of several atomic lines, in particular 5876Å, 3889Å, 5016Å and 4713Å have been measured as a function of time. There seems to be little or no difference between the time dependence of different atomic lines. Figures 2 and 3 show the time behaviour of the 5876Å and 5016Å lines as a function of time, both with and without heating of the electron gas by diathermy radiation at 2450 MHz. When the electron gas is heated, the recombination coefficient is reduced drastically and the recombination light is extinguished as shown by the fact that the spectral line intensity drops essentially to zero at the time the plasma excitation is cut off. Thus the curves with diathermy heating represent only the light due to direct excitation by beam electrons while the curves without diathermy heating show the light due to both direct excitation and recombination. It is therefore clear from Figs. 2 and 3 that, during the active discharge, approximately 80% of the 5016Å light results from direct excitation while the 5876Å light is the result mainly of recombination. As the exciting electron beam is cut off, there is an initial drop in the light intensity, due to removal of direct excitation, followed immediately by a pronounced rise as the electron gas cools thus increasing the recombination coefficient. Subsequently the recombination rate, and hence the light intensity, begin to fall as the electron density decreases.

In order to determine the radial light intensity distribution, measurements of the projected spectral line intensity profile were made by scanning the spectrometer across the tube. These measurements were made with time resolution using a gate length of 10 to 15 μs. The Abel inversion of these profiles was calculated by a computer program using a series expansion in either Legendre, Tchebycheff or Gegenbauer ($\alpha = 2$) orthogonal polynomials.[13, 14]

The resulting radial line intensity distributions from one extensive set of projected profiles, showed an initial change during the first 50 to 100 μs after which the radial distribution remained essentially constant for at least 2 ms. Thus the light intensity and electron density, measured as an average along a diameter of the plasma tube, can be referred to the values on the axis by a factor which remains constant from at least 100 μs to 2 ms.

To determine what this factor should be, the equations for non-linear diffusion[15] but with the recombination loss added[16] were solved on the computer for the case of zero magnetic field.

The resulting radial electron density distributions, $n(r)/n(0)$, for various values of the ratio of recombination loss to diffusion loss were related to the radial spectral line intensity distribution, $I(r)$, by the equation $I \propto \alpha(n)\, n^2$, where the recombination coefficient, $\alpha(n)$, used in the calculation could be two-body, three-body or the intermediate case of collisional-radiative recombination for some given electron temperature. When the resulting radial line intensity distributions are compared with each other, it is immediately seen that the shape of the distribution depends mainly on the ratio of recombination loss to diffusion loss and is relatively insensitive to the particular mechanism of recombination being considered. Furthermore, the needed correction factor, which is just the ratio of the electron density at the center to the density averaged along a diameter, is itself fairly insensitive to errors in the ratio, R, of recombination loss to diffusion loss. The resulting correction factor for the electron density was between 1.30 and 1.35. Referring to Fig. 4, it is difficult to see how it could be in error by more than 10%.

Comparison of the theoretical curves calculated under the steady state assumption, with experimental distributions measured in the afterglow can be justified by two arguments. Since the electron-neutral collision time is many orders of magnitude shorter than the time during which the electron density changes noticeably, we are therefore considering a case where only an adiabatic change occurs. Furthermore, in the theoretical calculation, the ratio of the equivalent source frequency $\nu_s = s/n$ (where s is the source term in units of $cm^{-3} sec^{-1}$ and n is the electron density in cm^{-3}), to the electron-neutral collision frequency has already been chosen very small ($\sim 10^{-6}$). Consequently it is thought that a comparison of the theoretical radial intensity distributions with the experimental ones gives a reasonable indication of the actual ratio of recombination loss to diffusion loss at the center of the plasma. In the analysis of the I (t) and n (t) curves, as will be seen later, one obtains an additional check on this ratio in terms of the ratio of y to D/Λ^2.

Measurements of the time dependent electron density, n (t), were made using a microwave interferometer at 35 GHz [17] the beam of which was collimated by absorbers to a circular cross section of 35 mm diameter. Thus the observed phase shift was a measure of the average electron density along a diameter of the plasma tube. Phase shifts of as low as one degree were detectable, corresponding to approximately 10^{10} electrons per cm^3.

The electron temperature, T_e, was measured by a pulsed Langmuir probe technique in which the probe was pulsed, once in each afterglow period, using a square pulse of approximate duration 10 μs

and of variable height. By manually varying the height of the pulse, a probe curve was thus traced out on an x-y oscilloscope, the trace being brightened during the flat top of the pulse applied to the probe. Such probe curves, taken in the steady state brush cathode plasma were compared with a spectroscopic determination of the electron temperature both from the relative light intensity of the high lines ($n = 10$ to $n = 21$) in the $n\,^3P \rightarrow 2\,^3S$ series, and from the intensity of the continuum beyond this series limit. Of the two, the continuum measurement was the more precise, with a precision of about ± 5% compared to approximately ±15% for the relative line intensity. The precision of the pulsed probe measurement was about ±5%. The electron temperatures found from the continuum measurements and the pulsed probe measurements agreed to within approximately 5%. Two 80-cm Leeds and Northrup spectrometers were used in tandem in order to reduce the scattered light so that these measurements could be made. Due to the low fractional duty cycle, time resolved spectroscopic measurements of the temperature using a pulsed discharge were not feasible.

Finally, measurements of the absorption of 3889Å and 5016Å radiation by the plasma, allowed an estimate of the densities of the $2\,^3S$ and $2\,^1S$ helium metastable atoms. A water-cooled helium capillary discharge was used as the light source. The technique used for measuring low fractional absorptions was similar to that of Phelps and Pack [18] and the limiting sensitivity of 2×10^{-4} was also essentially the same. Fractional absorptions as high as .24 were observed for the 3889Å line, corresponding to a $2\,^3S$ metastable density of approximately 2.6×10^{11} cm^{-3}, averaged along a diameter. Fractional absorption of 5016Å light was an order of magnitude lower than this and exhibited a faster time decay. The maximum observed

value corresponds to a 2^1S metastable density of 6×10^9 cm^{-3}. In calculating the metastable density from the fractional light absorption, gaussian line shapes were assumed for both the emission profile of the lamp and the absorption profile of the plasma, with the ratio, ρ, of the absorption width to emission width becoming a parameter of the equation (see the appendix). The solution of the equation shows that, for a constant fractional absorption, the variation in the calculated metastable density as ρ as is varied from .5 to 2.0 is less than a factor of 2. The data was analyzed assuming $\rho = 1$.

ANALYSIS OF DATA

In all of the following analysis, it is understood that the function n (t) used in the equations has already been corrected to the density at the center of the tube by the method outlined above.

The differential equations governing the concentration of the three major charged components of the plasma are, where a dot over a symbol indicates its time derivative, as follows:

$$\dot{n} = -\alpha(n) n [He^+] - \alpha_M(n)\, n [He_2^+] - \frac{D}{\Lambda^2} [He^+] - \frac{D_M}{\Lambda_M^2} [He_2^+]$$

$$+ \gamma [2^3S]^2 , \qquad (1)$$

$$\dot{[He^+]} = -\alpha(n)\, n [He^+] - \frac{D}{\Lambda^2} [He^+] + \gamma [2^3S]^2$$

$$-\delta [He]^2 [He^+] , \qquad (2)$$

$$\dot{[He_2^+]} = \delta [He]^2 [He^+] - \alpha_M(n)\, n [He_2^+] - \frac{D_M}{\Lambda_M^2} [He_2^+] . \qquad (3)$$

Furthermore, the atomic and molecular line intensities are given by

$$I_A = k_A \alpha (n)\, n\, [He^+] \tag{4}$$

and

$$I_M = k_M \alpha_M (n)\, n\, [He_2^+] \tag{5}$$

where, in general, k_A and k_M differ for each line considered and are to some extent temperature dependent. Other symbols used are the electron density, n; the atomic and molecular recombination coefficients expressed in two-body form, but actually without any assumption as to their n-dependence, $\alpha (n)$ and $\alpha_M (n)$ respectively; the atomic and molecular ambipolar diffusion coefficients, D and D_M; the corresponding diffusion lengths, Λ and Λ_M; and the rate coefficients, γ and δ, for the following reactions:

$$He\,(2^3S) + He\,(2^3S) \xrightarrow{\gamma} He^+ + e + He\,(1^1S) \tag{6}$$

and

$$He^+ + 2He \xrightarrow{\delta} He_2^+ + He. \tag{7}$$

Finally,

$$n = [He^+] + [He_2^+]\ . \tag{8}$$

Brackets indicate the densities of the reactant components.

We have calculated γ from the relation $\gamma = v\sigma$ using the value[19] of $\sigma = 5 \times 10^{-15}$ cm^2, which results in $\gamma = 5.8 \times 10^{-10}$ cm^3 sec^{-1}. The value of δ used[20] was 1.08×10^{-31} cm^6 sec^{-1}. These reaction rates depend on the neutral and ion temperatures but not on the electron temperature. On the other hand, the diffusion terms D/Λ^2 are less well known and, furthermore, depend on electron temperature and radial electron density distribution. Fortunately, in our case they are also small relative to the recombination loss term during the early afterglow.

If dissociative recombination also occurs, then the light intensities of Eqs. (4) and (5) must be rewritten as

$$I_A = k_A\,\alpha(n)\,n\,[He^+] + k_D\,\alpha_D(n)\,n\,[He_2^+] \tag{9}$$

and $$I_M = k_M\,\alpha_{CR}(n)\,n\,[He_2^+] \tag{10}$$

where $\alpha_D(n)$ is the dissociative recombination coefficient and α_{CR} is the collisional-radiative recombination coefficient for the He_2^+ ion. If we further assume that the production of atomic light is dominated by the dissociative process, then we may write

$$\frac{\dot{I}_A}{I_A} = \frac{\dot{\alpha}_{CR}}{\alpha_{CR}} + \frac{\dot{n}}{n} + \frac{[\dot{He_2^+}]}{[He_2^+]} \tag{11}$$

and

$$\frac{\dot{I}_M}{I_M} = \frac{\dot{\alpha}_{CR}}{\alpha_{CR}} + \frac{\dot{n}}{n} + \frac{[\dot{He_2^+}]}{[He_2^+]} \,. \tag{12}$$

The difference between these two equations gives

$$\frac{\dot{I}_M}{I_M} - \frac{\dot{I}_A}{I_A} = \frac{\dot{\alpha}_{CR}}{\alpha_{CR}} - \frac{\dot{\alpha}_D}{\alpha_D} \,. \tag{13}$$

If the assumed dissociative recombination is a two-body process so that $\dot{\alpha}_D/\alpha_D = 0$, then of necessity the right-hand side of the equation is less than or equal to zero. Measurements of the atomic and molecular light in one set of data show that the atomic light disappears faster than the molecular light by a factor of about 4 in the early afterglow (40 to 400 μs), diminishing to a factor of approximately 2 during the interval 1 to 2 ms. Thus the left-hand side of the equation is definitely positive and of the order of 10^3 sec^{-1}. The recombination coefficients on the right side have time derivatives only because of their dependence on the electron density. The collisional-radiative recombination coefficient is proportional to the electron density raised to a power between zero and one.

In the region of electron density and temperature of this experiment, one would expect the power to be closer to 1, so that $\dot{\alpha}_{CR}/\alpha_{CR} \sim \dot{n}/n$. Collins[21] has recently investigated the theory of collisional-dissociative recombination and finds a three-body dependence ($\alpha_D \propto n$) over a much wider range than for collisional-radiative recombination. No theory has been proposed which either predicts a dependence on n to a power greater than 1 or for which one could reasonably expect an n-dependence for dissociative recombination to a power higher than that for collisional-radiative recombination. Consequently we conclude that no dissociative recombination mechanism can play a dominant role in the afterglow of this experiment.

If the dominant recombination mechanism turns out to be that of collisional-radiative recombination, then one expects little or no difference between the recombination coefficients of the atomic and the molecular ion. In this case, then, a solution of Eq. (3) for the steady state shows that the molecular ion constitutes no more than about 20% of the total positive ion concentration during the early afterglow. For much of the data it is considerably less. If the molecular recombination coefficient should be as much as a factor of two higher, the equilibrium density would be further reduced. The end result is that, assuming a factor of two either way in the ratio of the molecular to atomic recombination coefficients, the weighted average recombination coefficient is not changed by more than ±15%. Since for most of the data the molecular ion concentration is even lower than 20%, the maximum error introduced by assuming the atomic and molecular coefficients to be the same is even less than 15%.

Under the assumptions that $\alpha(n) = \alpha_M(n)$ and, since they are small corrections, that $D/\Lambda^2 = D_M/\Lambda_M^2$, we can rewrite equations (1) through (5), using the definitions

$$y(t) = \alpha(n)\, n(t) \tag{14}$$

and

$$\Delta \equiv \delta [He]^2 = 135\, p^2 \tag{15}$$

where p is the neutral gas pressure in torr. The equations then become

$$\frac{\dot{n}}{n} = -y - \frac{D}{\Lambda^2} + \gamma \frac{[2^3S]^2}{n} \tag{16}$$

$$\frac{[\dot{He}^+]}{[He^+]} = -y - \frac{D}{\Lambda^2} - \Delta + \gamma \frac{[2^3S]^2}{[He^+]} \tag{17}$$

$$\frac{[\dot{He}_2^+]}{[He_2^+]} = \Delta \frac{[He^+]}{[He_2^+]} - y - \frac{D}{\Lambda^2} \tag{18}$$

$$\frac{\dot{I}_A}{I_A} = \frac{\dot{y}}{y} + \frac{[\dot{He}^+]}{[He^+]} = \frac{\dot{\alpha}}{\alpha} + \frac{\dot{n}}{n} + \frac{[\dot{He}^+]}{[He^+]} \tag{19}$$

and

$$\frac{\dot{I}_M}{I_M} = \frac{\dot{y}}{y} - \frac{[\dot{He}_2^+]}{[He_2^+]} \quad . \tag{20}$$

We have here neglected the term $\dot{k}_A/k_A$ in Eq. (19) and a similar one in Eq. (20) on the grounds that the dependence of k_A on T_e is not great and that the dependence of T_e on time is not very rapid.

The recombination coefficient can be extracted in three different ways. First of all, the n(t) measurement is alone sufficient to determine $\alpha(n)$ from Eqs. (14) and (16). There are two serious objections to this approach. First of all, we need prior knowledge as to the value of D/Λ^2 and, perhaps more serious, we require the determination

of the time derivative of n, as a function of time, a rather inaccurate procedure.

A second approach is to use both the I(t) and n(t) data, thus obtaining $\alpha(n)$ from the equation

$$\alpha(n) = \frac{I(t)}{n^2(t)} \quad \frac{y(t_o)\, n\,(t_o)}{I\,(t_o)} \tag{21}$$

where $y\,(t_o)$ is obtained from Eq. (16).

The starting time for the calculation, t_o, is always chosen so that the initial temperature and radial distribution changes which follow the discharge cutoff have already occurred and a new quasi-equilibrium has been reached. Typically, t_o was chosen to be 100 μs in the afterglow. In this second approach we can in principle determine D/Λ^2 from the difference between $\dot{n}/n$ at two different times, preferably widely separated. However, the exact value of D/Λ^2 so calculated will depend on which values of time are chosen, and averaging over-all values of time would become hopelessly involved. Determining $\dot{n}/n$ from the available data for a time late in the afterglow is at best inaccurate.

The third, and by far the most convenient approach, is to use the $I_A(t)$ measurement supplemented only by the values of n and $\dot{n}$ at time t_o. We pick a value of D/Λ^2 or, if $T_e(t)$ is known, a value of D/Λ^2 for $T_e = T_g$ where T_g is the temperature of the neutral gas. Neglecting changes in Λ^2, the function D/Λ^2 vs t is then determined since D is proportional to the electron temperature. By the solution of two successive differential equations, we then determine y (t) and α (t). Using Eq. (14), n (t) is also calculated. This calculated n (t) curve is then compared with the experimentally determined one and the whole calculation is repeated with different values of $D/\Lambda^2(T_g)$ until the best fit is found. In more detail, we proceed as follows. Substitute Eq. (17) into Eq. (19) thus obtaining the differential equation

$$\dot{y} - y^2 - yF(t) = 0 \tag{22}$$

where F(t) is the experimentally determined function

$$F(t) = \frac{\dot{I}_A}{I_A} + \frac{D}{\Lambda^2} + \Delta - \gamma \frac{[2^3S]^2}{[He^+]} \quad . \tag{23}$$

The relative sizes of these terms for this experiment are $\gtrsim 10^3$: $\sim 200/p$: $135\,p^2$: $\gtrsim 40$ where p is again the neutral gas pressure in torr. The last term will now be neglected and the solution of Eq. (22) then becomes

$$y(t) = \frac{I_A(t) \exp\left[\int_{t_o}^{t} \frac{D}{\Lambda^2}\, dt + \Delta\,(t - t_o)\right]}{\frac{I_A(t_o)}{y(t_o)} - \int_{t_o}^{t} I_A(t) \exp\left[\int_{t_o}^{t} \frac{D}{\Lambda^2}\, dt + \Delta\,(t - t_o)\right] dt} \quad . \tag{24}$$

The substitution of Eqs. (16) and (17) into Eq. (19) second form results in

$$\frac{\dot{\alpha}}{\alpha} = \frac{\dot{I}_A}{I_A} + 2y + 2\frac{D}{\Lambda^2} + \Delta \tag{25}$$

where we have again neglected the term in γ. Since y(t) is now known, we obtain as a solution of Eq. (25),

$$\alpha(t) = \frac{y(t_o)\, I_A(t)}{n(t_o)\, I_A(t_o)} \exp\left[2\int_{t_o}^{t} y(t)\, dt + 2\int_{t_o}^{t} \frac{D}{\Lambda^2}\, dt + \Delta\,(t - t_o)\right] \tag{26}$$

Finally,

$$n(t) = y(t) / \alpha(t) \,. \tag{27}$$

The initial condition of $y(t_o)$ is given by

$$y(t_o) = -\frac{\dot{n}(t_o)}{n(t_o)} - \frac{D}{\Lambda^2}\bigg|_{t_o} + \gamma \frac{[2^3S]^2}{n}\bigg|_{t_o} \tag{28}$$

where there is here somewhat less reason for neglecting the term in γ and also less inconvenience in keeping it. The accurate calculation of $\dot{n}(t_o)/n(t_o)$ is greatly helped, at least in the present experiment, by the convenient fact that from 100 μs to approximately 1 ms, the function $1/n(t)$ plots linearly against time. Thus, $\dot{n}(t_o)/n(t_o) = -n(t_o)$ (slope of the plot). Note that the slope of this plot does not equal the recombination coefficient, as was sometimes assumed in earlier work.

If a molecular line is also observed, we can obtain additional information by proceeding as follows. Equations (17) and (18) are substituted into the difference between Eqs. (19) and (20) to obtain

$$\frac{\left[He_2^+\right]}{n} = \frac{\Delta}{\frac{\dot{I}_M}{I_M} - \frac{\dot{I}_A}{I_A}}, \qquad (29)$$

still under the assumption $\alpha(n) = \alpha_M(n)$. For the one case where data were available to allow the use of this equation, the values were $[He_2^+]/n$ equal to .092 in the early afterglow (40 μs to 400 μs) and approximately .27 during the interval 1 ms to 2 ms, in good agreement with estimates mentioned above based on Eq. (3) in the steady state.

To a first approximation in Eqs. (24) and (26), we can assume that D/Λ^2 is a constant, thus ignoring its dependence on the electron temperature. The value of D/Λ^2 then becomes the time average over the total interval being studied. Even in this approximation, agreement of calculated n(t) with experimentally measured n(t) to within experimental error can be obtained from 100 μs to 11 ms in the afterglow. This agreement is shown in Figure 5 for one set of data. The ratio $\alpha(n)/n$ is then plotted vs. n in Figure 6 superimposed on a family of curves representing predictions of the collisional-radiative recombination theory[5]. The corresponding time in the afterglow and measured

electron temperature are indicated by arrows. The agreement is good but it remains to be explained why the electron temperature remains elevated during a long period in the afterglow after falling abruptly by a factor of 1.3 to 2 immediately following plasma excitation cut-off.

Consideration of the continuity equation for the density of He (2^3S) metastables in the light of its measured time dependence in the afterglow, forces us to include a term of the form $k^* n(t)$ corresponding to collisional de-excitation by electrons, hence,

$$\frac{\dot{[2^3S]}}{[2^3S]} = \beta[2^1S]\frac{n(t)}{[2^3S]} + .67\,\frac{y(t)\,[He^+]}{[2^3S]} - \frac{D}{\Lambda^2} - \gamma\,[2^3S]$$

$$-k\,[He]^2 - k^*\,n(t) \qquad (30)$$

where the term in β is due to the reaction

$$He(2^1S) + e \xrightarrow{\beta} He\,(2^3S) + e + .79\ eV, \qquad (31)$$

the next two terms are the contributions of recombination into triplet levels and diffusion respectively, the term in γ is due to loss by metastable-metastable collisions (Eq. 6), and that in k to loss by the reaction

$$He\,(2^3S) + 2\,He \xrightarrow{k} He_2\,(2^3\Sigma^+_u) + He\,(1^1S). \qquad (32)$$

Using the values $\beta = 3.5 \times 10^{-7}\ cm^3\,sec^{-1}$ and $k = 2.5 \times 10^{-34}\ cm^6\,sec^{-1}$ given by Phelps[22], we arrive at the following approximate magnitudes for the terms of Eq. (30) during the early afterglow of this experiment:

$$-2 \times 10^3 = +\lesssim 200 + 4 \times 10^{-3} - 165 - 110 - .26 - 6 \times 10^{11}\,k^*$$

Thus the approximate magnitude of k^* must be $10^{-8}\ cm^3\ sec^{-1}$. Since $k^* = v\sigma$, we arrive at a cross section $\sigma \sim 10^{-15}\ cm^2$ for the collisional de-excitation of the He (2^3S) metastable by electrons.

If, instead of this process, we assume de-excitation by collisions with the neutral gas resulting in a term k^* [He], we cannot obtain the measured time dependence of the 2^3S metastable density. Loss by collisions with He^+ or He_2^+ ions or with other 2^3S metastables, resulting in the terms k^* [He^+], k^* [He_2^+] or k^* [2^3S], cannot, because of the lower velocity of these particles, yield a term of the required magnitude without resorting to cross sections larger than the maximum permissable. It seems therefore that only de-excitation by super elastic electron collisions is adequate to explain the experimental observations. This mechanism results in an electron of energy 19.8 eV, and is therefore possibly also instrumental in maintaining the electron temperature during the afterglow.

Other possible mechanisms which can contribute energy to the electron gas are He (2^3S) metastable-metastable collisions, which release an electron of about 15 eV energy, transformation from 2^1S to 2^3S metastables by superelastic electron collisions releasing .79 eV, and the collisional-radiative rrecombination process itself. In this later process, an electron, newly attached to a positive ion in a very high level, gradually loses energy to free electrons until it reaches a level where radiative transitions downward become favored relative to collisional transitions.[23]

For our conditions of electron density and electron temperature, this occurs at a level of principal quantum number 5 or 6, lying about .4 eV below the continuum. Thus for each recombination event, approximately .4 eV of energy should be transfered to the electron gas. The differential equation describing these processes is

$$\frac{d}{dt} kT_e = -2\frac{m}{M}\nu_m(kT_e - kT_g) + .67\alpha(n)\, n\, V_{ion}(n)$$

$$+ 15\gamma\frac{[2^3S]^2}{n} + 19.8\, k^*[2^3S] + .79\beta[2^1S] \qquad (33)$$

in units of eV electron $^{-1}$ sec $^{-1}$. Here T_g is the temperature of the neutral gas, and ν_m is the electron-neutral collision frequency.[24]

The time constants involved in this equation are all short ($\sim 10^{-6}$ to 10^{-5} sec) but it is known from the pulsed probe measurements that the electron temperature varies only rather slowly following its initial rapid drop. A quasi-equilibrium must therefore be reached and we may neglect the time derivative in Eq. (33). Defining the ratio $\Theta = T_e/T_g$ and using $\nu_m = 1.8 \times 10^8 \sqrt{\Theta}$, one thus obtains

$$\sqrt{\Theta}\,(\Theta - 1) = .52 \times 10^{-3}\, y(t)\, V_{ion}(n) + .69 \times 10^{-11} \frac{[2^3S]^2}{n}$$

$$+ 1.5 \times 10^{-10} [2^3S] + 2.2 \times 10^{-10} [2^1S]. \qquad (34)$$

Using typical observed values of the metastable densities at 100 μs, $[2^3S] \simeq 1 \times 10^{11}$ cm $^{-3}$ and $[2^1S] \simeq 3 \times 10^9$ cm $^{-3}$, it follows from Eq. (34) that if all the energy of the metastable-metastable and metastable-electron collisions were coupled efficiently to the electron gas, the electron temperature would be very high, above 4000°K. Consequently only a relatively small fraction of this energy must go into heating the electron gas. Most of the energy is probably lost in collisions with neutral atoms. Furthermore, since an electron of .79 eV can more easily share its energy with the electron gas than can one of 15 or 19.8 eV, it is quite possible that heating by conversion of 2^1S to 2^3S metastables might be a mojor electron temperature maintaining mechanism in the afterglow.

The rate of formation of metastables controls the metastable density in the afterglow to a large extent, and consequently all of the

above heating processes are dependent, either directly or indirectly, on the recombination rate. For high electron densities, the recombination rate is proportional to n^3, therefore one might expect the rate of energy input per electron to increase rapidly as the electron density is raised above 10^{12} cm $^{-3}$. If so, then it is clear that a helium plasma, in near equilibrium and of high electron density, must of necessity have an electron temperature several times room temperature, even during much of the afterglow.

SUMMARY

It is shown that dissociative recombination cannot play a major role in the decay of the plasma of this experiment. Analysis of spectral line intensity and electron density measurements as a function of time allow the determination of the coefficient for recombination of atomic ions with electrons. Simultaneous measurements of the electron temperature then permit a comparison with the theory of collisional-radiative recombination. Agreement is obtained to within a factor of approximately two in the value of $\alpha(n)/n$ or a factor of approximately 1.15 in the electron temperature.

Use of the measured time dependence of the 2^3S metastable density in the continuity equation suggests that the dominant loss mechanism for 2^3S metastables is collisional de-excitation by electrons with a cross section of the order of 10^{-15} cm^2.

A study of the possible heating mechanisms together with measurements of the metastable atom densities, suggest that the major heating mechanisms in the early afterglow involve super-elastic collisions of electrons with the metastable atoms. An appreciable contribution to heating should also result from the collisional-radiative recombination process itself. Since these heating mechanisms are controlled directly or indirectly by

the recombination rate, it is suggested that the existence of a dense ($\gtrsim 10^{12}$ cm $^{-3}$) helium plasma, with electrons at essentially room temperature, is a fiction. The recombination process itself will assure an elevated electron temperature until the electron density has decreased.

ACKNOWLEDGEMENTS

The author wishes to acknowledge the valuable contributions of Dr. Robert S. Powers who collaborated on the pulsed probe technique, and Dr. Arthur L. Schmeltekopf who assisted with the spectroscopic electron temperature measurements. The contribution of R. W. Miles in constructing many of the specialized circuits as well as the contributions of other members of the Radio Plasma Section are gratefully acknowledged.

This work was supported by the Advanced Research Projects Agency.

APPENDIX

The relation is here calculated for the fractional spectral line absorption, A, as a function of metastable atom density for various values of the ratio, ρ, of the absorption line width to the emission line width of the light source assuming both line shapes are Gaussian. It is furthermore assumed that the slit of the spectrometer is open far enough that all of the emission and absorption lines are observed. The transmitted light, $I_t(x)$, can be written as

$$I_t(x) = I(x) \exp[-k(x)\, l] \tag{A-1}$$

where $x \equiv \lambda - \lambda_r$, $k(x)$ is the absorption coefficient, and l is the distance through the absorbing medium. The source and absorption line profiles are given by

$$I(x) = \frac{I_o}{\sqrt{2\pi}\,\sigma_e}\, e^{-x^2/2\sigma_e^2} \tag{A-2}$$

and

$$k(x) = K_o\, e^{-x^2/2\sigma_a^2} \tag{A-3}$$

where I_o is given by the integral of Eq. (A-2) over all x from $-\infty$ to $+\infty$. The total fractional absorption, integrated over the whole line is given by

$$A = 1 - \frac{\int_{-\infty}^{+\infty} I(x)\, e^{-k(x)\, l}\, dx}{I_o}\,. \tag{A-4}$$

Expanding $e^{-k(x)l}$ of Eq. (A-4) in a Taylor series and substituting Eq. (A-2) and (A-3), we then integrate to obtain

$$A = \sum_{n=1}^{\infty} (-1)^{n-1} \frac{K_o^{\,n}\, l^n\, \sigma_a}{n!\,\sqrt{\sigma_a^2 + n\sigma_e^2}}\,. \tag{A-5}$$

Mitchell and Zemansky[25] point out that the integral over an absorption line is constant irrespective of the absorption line width and is directly proportional to the total number of absorbing atoms per cm^2 in the optical path. This leads to the expression

$$K_o \equiv \frac{e^2}{mc^2} \, 2\sqrt{\pi}\sqrt{\ln 2} \, \frac{c}{\Delta\nu_a} \, fN \qquad \text{(A-6)}$$

which when substituted in Eq. (A-5) results in

$$A = \sum_{n=1}^{\infty} (-1)^{n-1} \, F^n / \, n! \, \rho^{n-1} \sqrt{\rho^2 + n} \qquad \text{(A-7)}$$

where

$$F \equiv \frac{e^2}{mc^2} \, 2\sqrt{\pi}\sqrt{\ln 2} \, \frac{c}{\Delta\nu_e} \, lfN \, , \qquad \text{(A-8)}$$

$$\rho \equiv \frac{\Delta\nu_a}{\Delta\nu_e} = \frac{\sigma_a}{\sigma_e} \, , \qquad \text{(A-9)}$$

and $\Delta\nu$ is the half width at half maximum of the emission line. Expression (A-7) was solved on the computer for various values of F and ρ. The results are plotted in Figure 7.

REFERENCES AND FOOTNOTES

1. M. A. Biondi and S. C. Brown, Phys. Rev. 76 1697 (1949); Johnson, McClure, and Holt, Phys. Rev. 80 376 (1950); D. E. Kerr, Bull. A.P.S. 5 372 (1960) Final Summary Report (July 31, 1960) unpublished; M. C. Sexton and J. D. Craggs, J. Electronic Control 4 493 (1958); H. J. Oskam, Phillips Res. Rep. 13 419 (1958); C. L. Chen, C. C. Leiby and L. Goldstein, Phys. Rev. 121 1391 (1961).
2. E. P. Gray and D. E. Kerr, Annals of Physics 17 276 (1962).
3. K.-B. Persson, Phys. Rev. 106 191 (1957).
4. D. R. Bates, Phys. Rev. 77 718 and 78 492 (1950); M. A. Biondi, Phys. Rev. 82 962L (1951).
5. D. R. Bates, A. E. Kingston and R. W. P. McWhirter, Proc. Roy. Soc. 267A 297 (1962), 270A 155 (1962); D. R. Bates and A. E. Kingston, Proc. Phys. Soc. 83 43 (1964).
6. E. E. Ferguson, F. C. Fehsenfeld and A. L. Schmeltekopf, Phys. Rev. 138 A381(1965).
7. R. W. Motley and A. F. Kuckes, Proc. Fifth Int. Conf. on Ion in Gases, Munich p. 651, North-Holland Publ. Co. Amsterdam (1962); E. Hinnov and J. G. Hirschberg, Phys. Rev. 125 795 (1962).
8. C. B. Collins, W. B. Hurt, and W. W. Robertson, Proc. 3rd. Int. Conf. on Elec. and Atomic Collisions, London 1963, North-Holland Publ. Co. Amsterdam (1964) p. 517; F. E. Niles and W. W. Robertson, J. Chem.Phys. 40 2909 (1964); F. Robben, W. B. Kunkel and L. Talbot, Phys. Rev. 132 2363 (1963).
9. D. R. Bates and A. E. Kingston, Proc. Roy. Soc. A279 32 (1964).
10. K.-B. Persson, N.B.S. Rpt. 8452 (Sept. 15, 1964); J. Appl. Phys. to be pub. (Oct. 1965).

11. That this is so has been confirmed by performing an Able inversion of a 5016 Å light intensity profile taken while the electron temperature was raised by a shining diathermy radiation on the plasma. Thus the recombination light was removed and only 5016 Å light from direct excitation by the electron beam was observed.
12. F. J. Norton, J. Amer. Ceramic Soc. 36 90 (1953).
13. C. H. Popenoe and J. B. Shumaker, to be published.
14. E. R. Mosburg, Jr. and M. S. Lojko, to be published.
15. K.-B. Persson, Phys. Fluids 5 1625 (1962); E. R. Mosburg, Jr. and K.-B. Persson, Phys. Fluids 7 1829 (1964).
16. E. R. Mosburg, Jr., to be published.
17. A. J. Estin and M. M. Anderson, to be published.
18. A. V. Phelps and J. L. Pack, Rev. Sci. Instr. 26 45 (1955).
19. A. V. Phelps and J. P. Molnar, Phys. Rev. 89 1202 (1952) Modified by a factor of two according to calculations by E. C. Zipf, Jr.
20. E. C. Beaty and P. L. Patterson, 137 A346 (1965).
21. C. B. Collins, to be published Phys. Rev.
22. A. V. Phelps, Phys. Rev. 99 1307 (1955).
23. S. Byron, R. C. Stabler and P. I. Bortz, Phys. Rev. Let. 8 376, 497E (1962).
24. The predominant electron collisions are still those between electrons and neutral atoms. The frequency of electron-ion collisions is lower by a factor of five than that of electron-neutral collisions.
25. Mitchell and Zemansky, "Resonance Radiation and Excited Atoms" Macmillan 1934, equation 35.

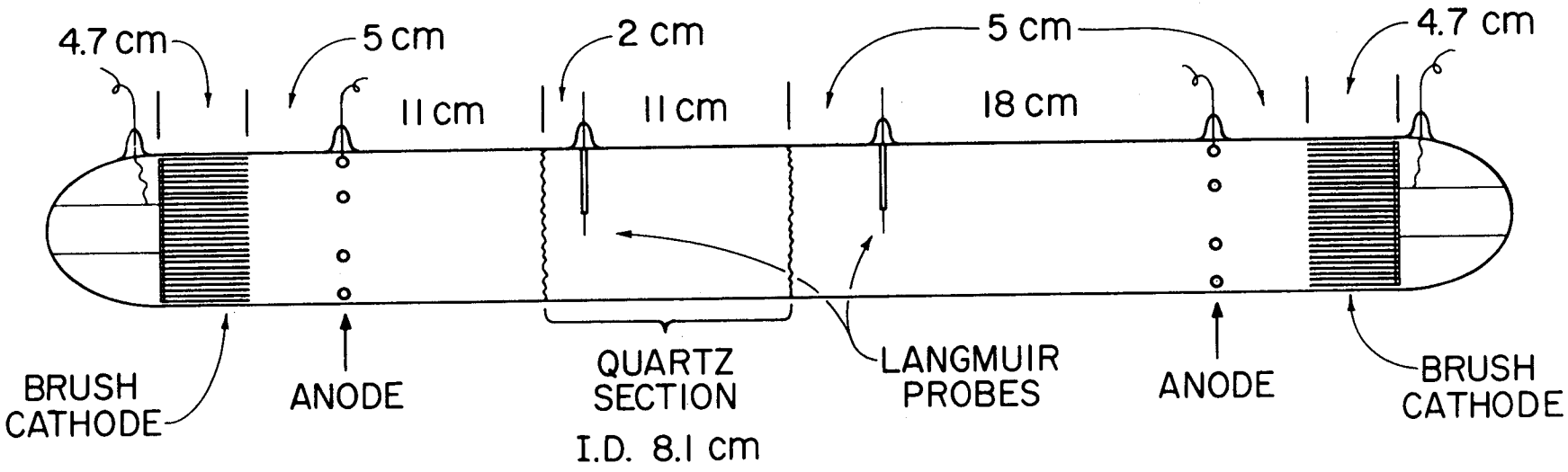

Fig. 1 Diagram of the plasma tube.

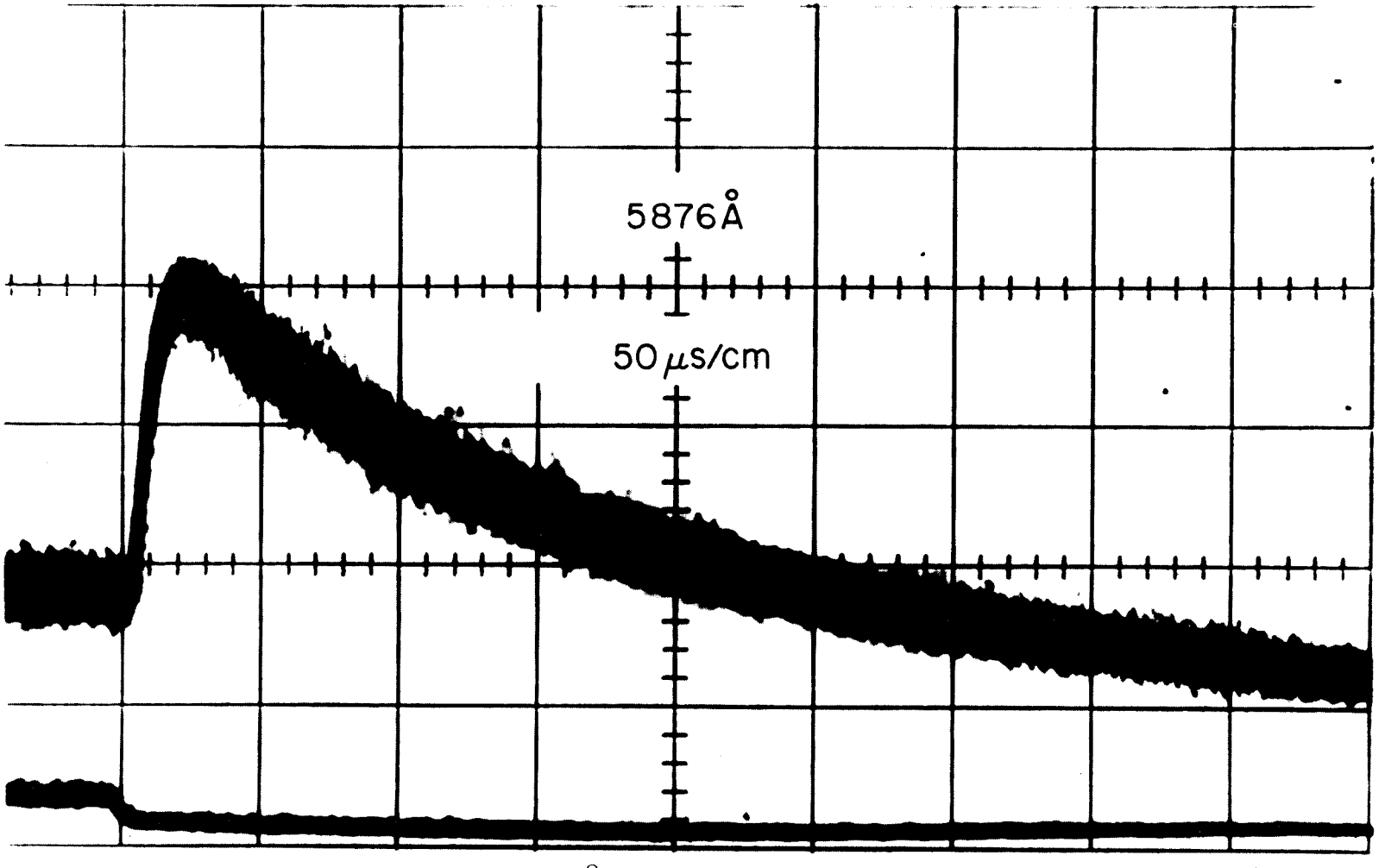

Fig. 2 Intensity of the 5876Å line of atomic helium as a function of time, 50 μs/cm. The top trace is without external heating of the electrons. The bottom trace is with the recombination light quenched by diathermy radiation at 2450 MHz. In this latter case the light intensity is essentially zero after cut-off of the plasma excitation.

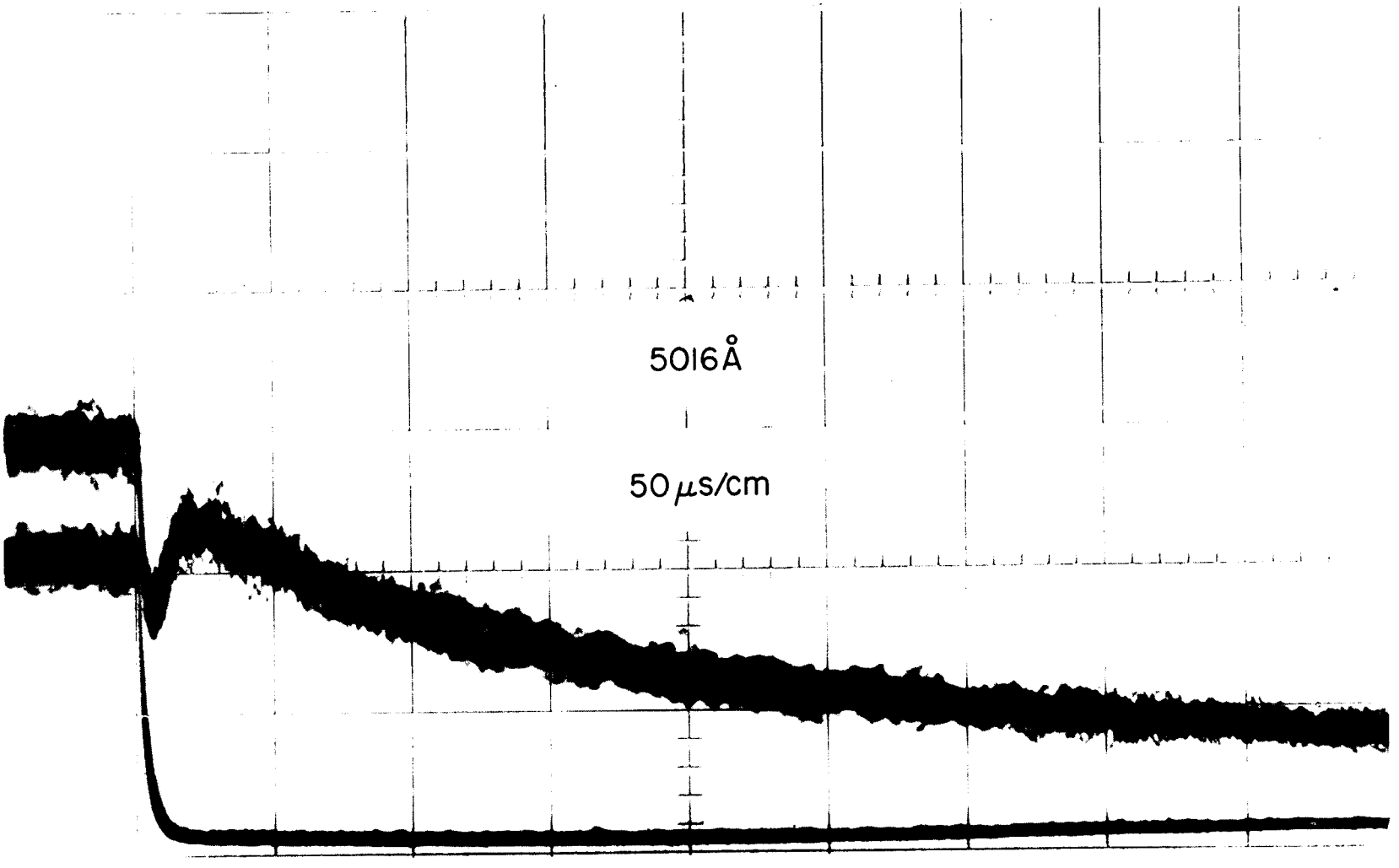

Fig. 3 Intensity of the 5016Å line of atomic helium as a function of time, 50 μs/cm. As in Figure 2, the top and bottom traces are respectively without and with microwave quenching of the recombination light.

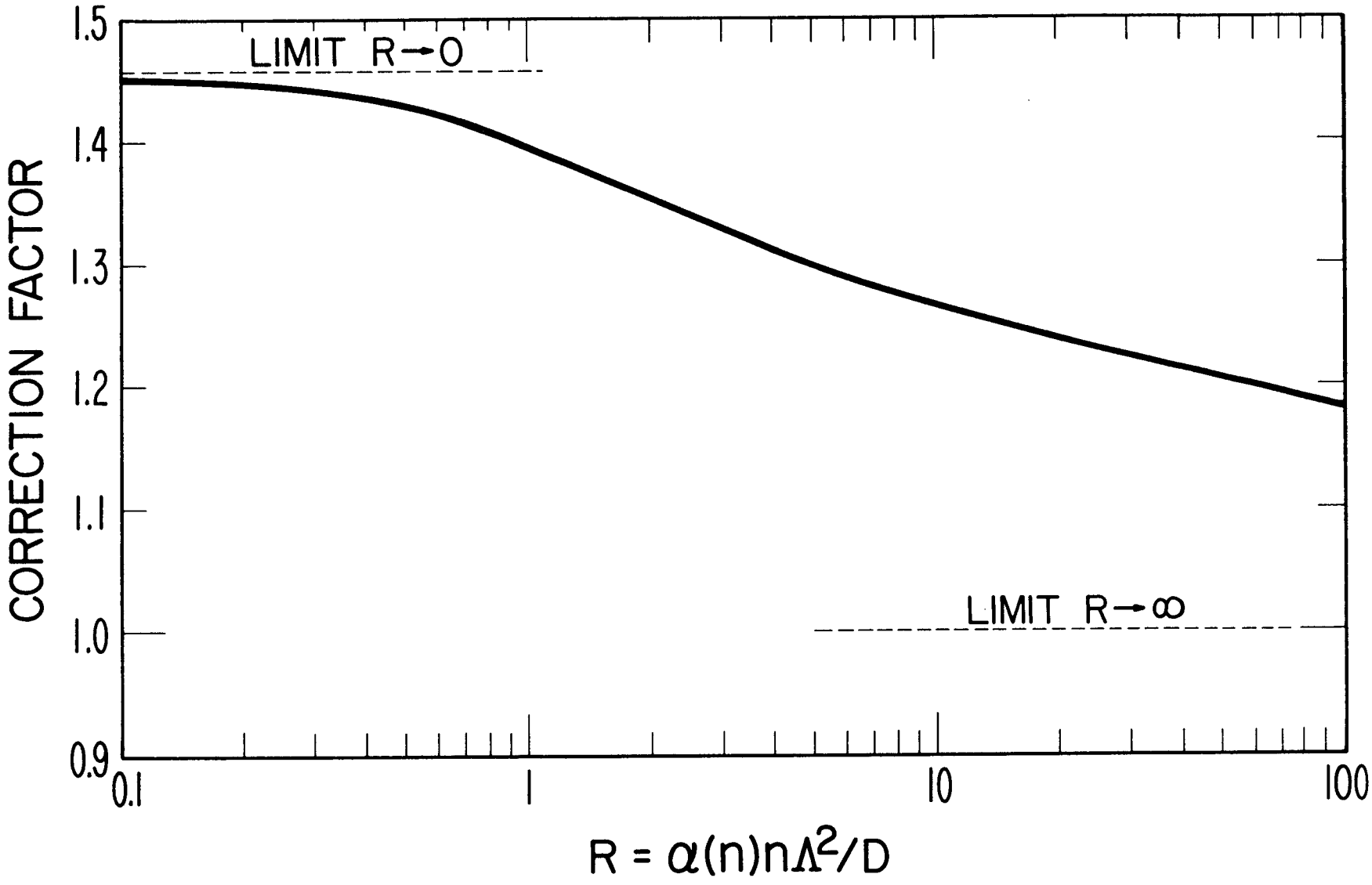

Fig. 4 Correction factor to be applied to the electron density averaged along a radius, in order to obtain the electron density at the center of the tube. It is plotted as a function of the ratio of recombination loss rate to diffusion loss rate, at the center of the plasma.

B-54470

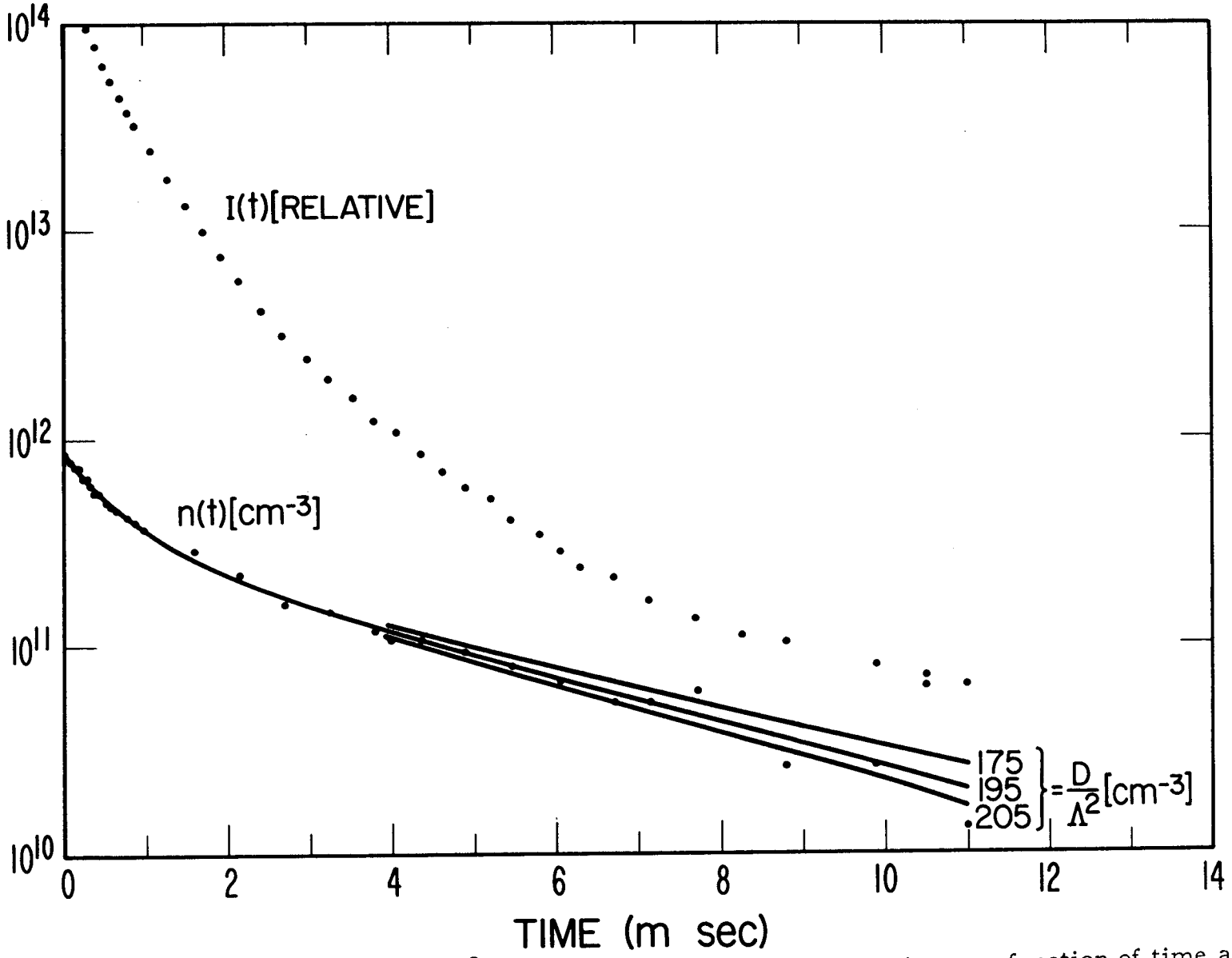

Fig. 5 Experimental 5876Å light intensity and electron density as a function of time are indicated by dots. The lines are calculated n(t) curves and show the type of fit to experimental n(t) which is possible.

B- 54554

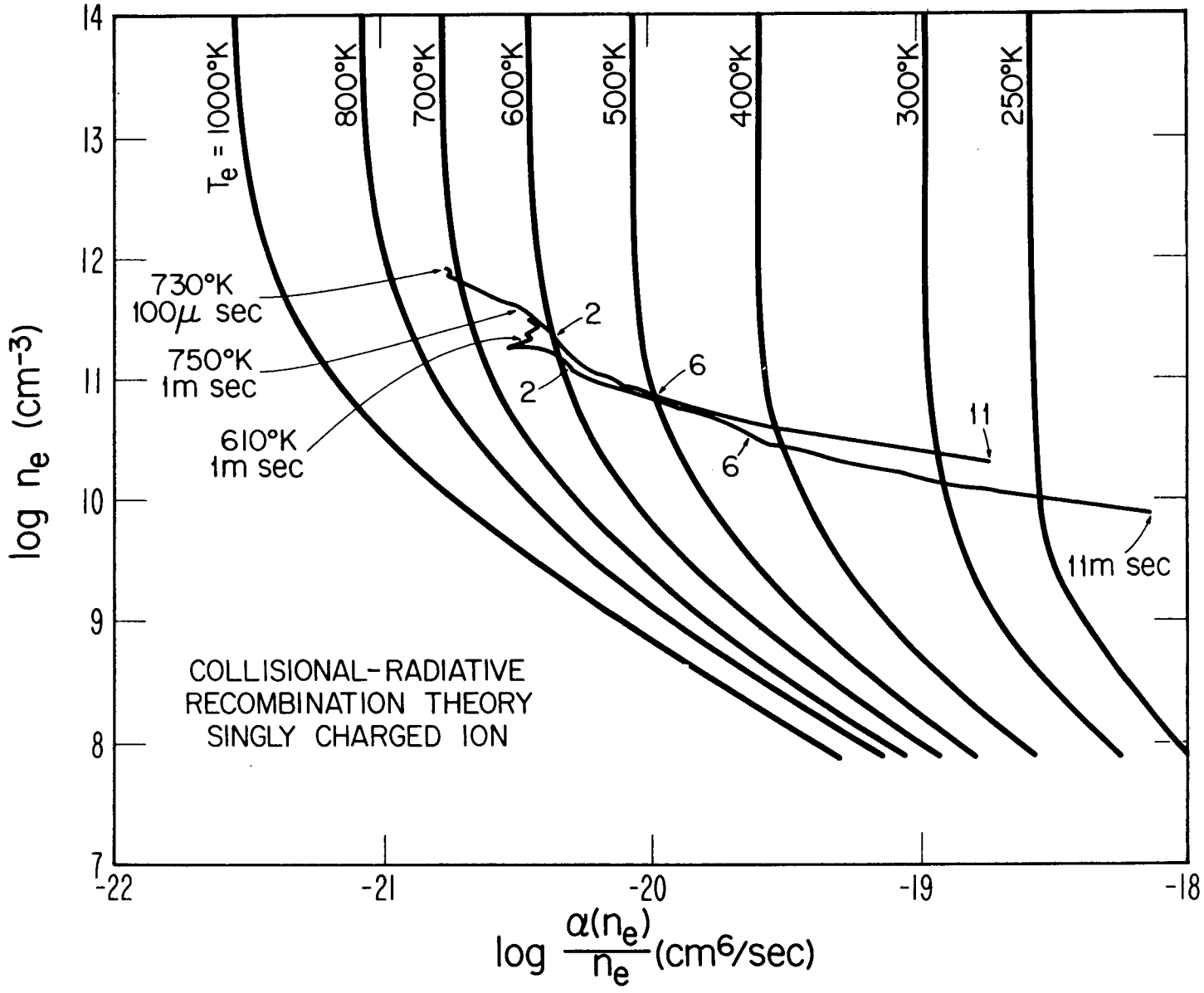

Fig. 6 Experimentally determined α(n)/n is plotted vs. n, superimposed on a family of curves indicating the predictions of collisional-radiative recombination theory.

B- 54553

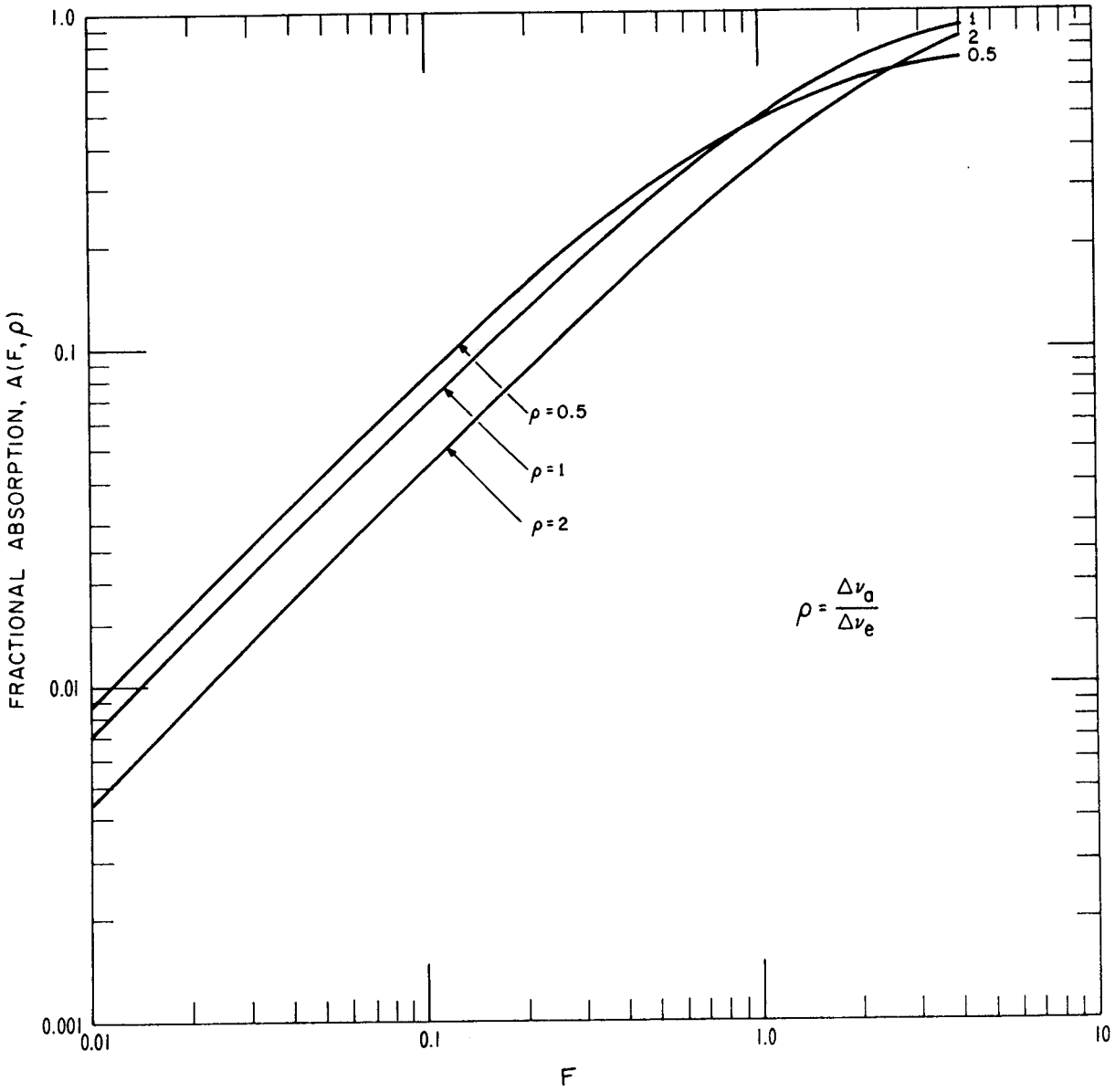

Fig. 7 Fraction absorption as a function of ρ, the ratio of absorption line width to emission line width, and the quantity F which is proportional to the density of absorbing atoms.

B-55354